THE JOURNAL OF PHYSICAL CHEMISTRY Letters

Letter

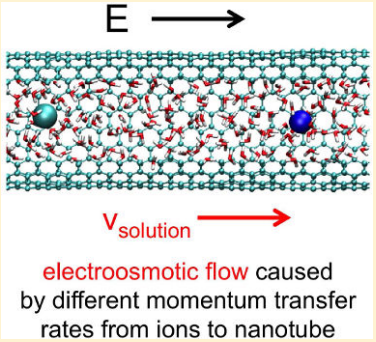
pubs.acs.org/JPCL

Molecular Friction-Induced Electroosmotic Phenomena in Thin Neutral Nanotubes

Lela Vuković,[†] Elizabeth Vokac,[†] and Petr Král*[,†,‡]

[†]Department of Chemistry and [‡]Department of Physics, University of Illinois at Chicago, Chicago, Illinois 60607, United States

ABSTRACT: We reveal by classical molecular dynamics simulations electroosmotic flows in thin neutral carbon (CNT) and boron nitride (BNT) nanotubes filled with ionic solutions of hydrated monovalent atomic ions. We observe that in (12,12) BNTs filled with single ions in an electric field, the net water velocity increases in the order of Na^+ < K^+ < Cl^-, showing that different ions have different power to drag water in thin nanotubes. However, the effect gradually disappears in wider nanotubes. In (12,12) BNTs containing neutral ionic solutions in electric fields, we observe net water velocities going in the direction of Na^+ for (Na^+, Cl^-) and in the direction of Cl^- for (K^+, Cl^-). We hypothesize that the electroosmotic flows are caused by different strengths of friction between ions with different hydration shells and the nanotube walls.



SECTION: Liquids; Chemical and Dynamical Processes in Solution

In recent years, molecular transport was intensively studied in silicon,[1] polycarbonate,[2] PMMA,[3] bio-organic and bioinorganic nanopores,[4,5] carbon (CNT)[6−14] and boron nitride (BNT) nanotubes,[15] porous graphene[16,17] and nanotubes,[18] and other synthetic nanopores. The molecular transport in nanochannels can be driven by electric fields,[19] pressure,[20] osmotic pressure,[21] and concentration gradients[22] and controlled by the pore size,[23,24] shape,[25] chemical functionalization,[2,13,26] pH,[27] and other means.

Electrokinetic phenomena, such as electrophoretic and electroosmotic flows (EOFs), have been thoroughly studied in nanopores.[28,29] In electrophoretic phenomena, charged molecules driven by external electric fields drag solvent molecules,[30] while the surrounding fluid remains largely quiescent (bulk).[31] In electroosmotic phenomena, flows of ionic solutions in channels are driven by external electric fields.[32] Typically, one type of ion is more or less stabilized at the channel walls, while the other one is free to move and drag the solvent.[33−35] EOF can also occur in nanopores[19,36] and nanotubes[11,37−44] with charged walls or chemical groups attached at the ends, where oppositely charged ions cannot enter or move through the channels in the same way.

Charged solid surfaces placed in ionic solutions induce the formation of electric double layers (EDLs).[32] Recently, it was shown that EDLs can also exist at the walls of neutral and nonpolar nanochannels[45−47] due to a different behavior of the oppositely charged ions in water monolayers adjacent to the walls. When electric fields were applied along channels with nanoscale dimensions, the velocities of the molecular components develop parabolic velocity profiles where different ions are moving with different speeds due to different distances from the well, which ultimately leads to EOF.[46,47] However, such effects were not reported in ultrathin channels with plug-like velocity profiles.[48] Here, we examine by classical molecular dynamics (MD) simulations the possible presence of the electric-field-driven flow of ionic solutions in CNTs and BNTs that lack Poiseuille flow but are known to have an extremely fast water transport due to a small friction of the fluid with the nanotube walls.[48]

Studied Systems. We study EOF in (12,12) and (16,16) single-wall neutral CNTs and BNTs, with diameters of $d \approx 1.6$ and 2.2 nm, respectively, filled with ionic solutions of monovalent (Na^+, K^+, and Cl^-) ions. Small ions, with tightly bound hydration shells, might not be able to enter narrow CNTs[49,50] and BNTs.[15,51,52] However, they may enter these nanotubes at higher ion concentrations.[53] The critical diameter of nanopores necessary for the entrance of individual hydrated Na^+ ions is $d \approx 7$ Å, which for the armchair (n,n) CNTs corresponds to the (7,7) CNT.[54] KCl solutions with concentrations $c > 0.01$ M show almost no rejection of ions by double-wall CNTs with the internal diameter of $d \approx 1.6$ nm and carboxylic groups at the tube ends.[53] Ions should be able to enter the (12,12) and (16,16) nanotubes at the used ion concentrations of $c = 0.05-0.15$ M.

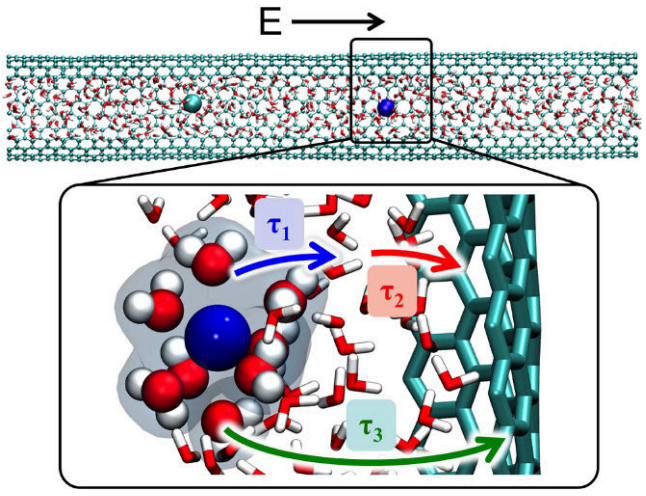
In our simulations, we neglect the polarizability of the used armchair (metallic) CNTs and BNTs and treat them as model nanochannels with a fixed polarity. We describe the electric-field-driven flow by NAMD[55,56] and the CHARMM27 force field,[57] where we add the nanotube force field parameters.[8,9] While carbon atoms in CNTs are neutral, B and N atoms in BNTs are chosen to have partial charges $q_B = -q_N = e$.[9,58]

In Chart 1, we show a unit cell of one model system formed by the (12,12) CNT of a length of $l \approx 10$ nm, filled with $N_w \approx 400$ water molecules (mass density of $\rho \approx 1$ g/cm^3) and one

Received: April 16, 2014
Accepted: May 29, 2014
Published: May 29, 2014

 © 2014 American Chemical Society dx.doi.org/10.1021/jz500761s | J. Phys. Chem. Lett. 2014, 5, 2131−2137

Chart 1. Electric-Field-Driven Solutions in Nanotubes[a]



[a](Na^+, Cl^-) pair solvated in $N_w \approx 400$ water molecules inside of a (12,12) CNT of length $l \approx 10$ nm; the ionic solution is driven by an electric field $E = 0.11$ V/nm (top). A scheme for the hydrated ion momentum dissipation in the studied systems, characterized by the characteristic relaxation times τ_1, τ_2, and τ_3 (bottom). The hydrated ion (gray cloud) passes momentum in τ_1 to free water, which passes in τ_2 to the nanotube. Alternatively, the hydrated ion passes its momentum in τ_3 directly to the nanotube.

pair of hydrated (Na^+, Cl^-) ions. All of the studied systems contain either single ions or single ion pairs within the nanotube segment. In the simulations, we model infinite nanotubes by positioning the nanotube segments inside of periodic cells, described by an *NVT* ensemble, with electrostatic periodic boundary conditions applied.[59] The temperature is held at $T = 300$ K by a small Langevin damping of $\gamma_{Lang} = 0.01$ ps^{-1} in order to avoid unphysical losses of momenta.[8,9] The ionic solution is driven by an electric field of $\mathcal{E} = 0.11$ V/nm applied along the nanotube (linear regime). The time step is set to 2 fs, and the coordinates are saved every 500 fs.

Systems with Single Ions. We start to model a field-driven transport of *single* hydrated Na^+, Cl^-, or K^+ ions in the (12, 12) and (16, 16) CNTs and BNTs, where the drag conditions are set as those in Chart. 1. In each system, the field-driven ion translates through the nanotube and drags water, and a steady-state flow is reached by friction of the ion and all of the water molecules with the freely vibrating nanotube walls (held at the tube ends). We equilibrate the systems for 1 ns and stabilize their steady-state flow for at least 2 ns (hydration shell water molecules exchange on the picosecond time scale), with the electric field applied, before we start to collect the simulation data.

We calculate the average velocities of the ions, v_i, water, v_w, and $\Delta v_i = v_i - v_w$, from

$$v_{i/w} = \frac{1}{N_t N_{i/w}} \sum_{k=1}^{N_t} \sum_{l=1}^{N_{i/w}} v_{kl} \quad (1)$$

Here, N_t is the number of time frames, $N_{i/w}$ is the number of ions or water molecules present in the system, and v_{kl} is the instantaneous velocity of the lth ion or water oxygen in the time frame k.

Table 1 shows the average velocities of ions, v_i, and water, v_w, obtained in 25−50 ns long trajectories. The velocities range from 10 to 88 nm/ns, in dependence of the ion and nanotube type. Our data show that ions have different velocities in different nanotubes, with the velocities (magnitudes) increasing in the order of $Na^+ < K^+ < Cl^-$. Interestingly, the same trend is also observed for water velocities, v_w, in Figure 1, where we plot the time dependence of the number of water molecules N_w passing through the (12,12) BNT, when driven by the single Na^+, K^+, or Cl^- ions. The plotted number of water molecules passing through the (12,12) BNT increases steadily with only small fluctuations, indicating that the observed differences are not due to fluctuations. In other nanotubes, water velocities differ less.

Table 1. Average Velocities of Cations and Anions (v_i) and Water Molecules (v_w), Velocities of the Ions with Respect to Water (Δv_i), and Electroosmotic Drag Coefficients of Ions (K_i) in Different Nanotubes, Obtained in 25−50 ns Long Simulations

v [nm/ns]	v_i	v_w	Δv_i	K_i
Na^+/C12[a]	83.2	77.2	6.0	371.2
B12	22.9	15.8	7.1	296.7
C16	51.6	41.9	9.7	649.6
B16	21.4	10.6	10.8	421.0
K^+/C12	87.6	77.4	10.2	353.4
B12	28.5	17.2	11.3	259.5
C16	56.1	42.2	13.9	601.8
B16	25.7	10.9	14.8	360.5
Cl^-/C12	−88.4	−78.7	−9.7	356.1
B12	−29.0	−18.0	−11.0	266.9
C16	−56.8	−41.9	−14.9	590.1
B16	−25.6	−11.0	−14.6	365.2

[a]C12 and C16 denote (12,12) and (16,16) CNTs, while B12 and B16 denote (12,12) and (16,16) BNTs, respectively.

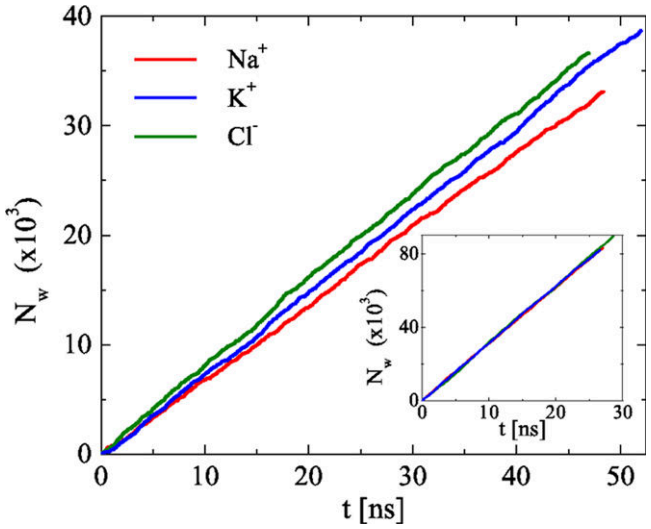


Figure 1. Time dependence of the number of water molecules (N_w) passed through (12,12) BNT and (12,12) CNT (inset) in systems with single solvated Na^+, K^+, or Cl^- ions.

Despite the fact that different ions have different velocities, v_i, they must gain and pass in steady-state flow the same momentum to the system (same fields) and, in principle, drag water at the same speed (with water molecules in front of the ion likely being slightly faster and water molecules behind the ion being slightly slower). We hypothesize that the different

dx.doi.org/10.1021/jz500761s | J. Phys. Chem. Lett. 2014, 5, 2131−2137

observed water drag velocities are related to the fact that different ions pass their momentum to water and nanotubes differently, that is, at different relative dissipation rates.

Simple Model of the Water Drag. We first build a simple qualitative model to explain the water drag velocity in different nanotubes (Table 1), without trying to capture the effect of the ion type. The ion is driven by a force of $F_{drive} = \dot{p}_{drive} = q\mathcal{E}$. In a steady state, the average velocity of the ion is constant because the driving force is balanced by a frictional force, which on average has equal size but opposite orientation. The momentum acquired by the ion from the field is continuously passed to the nanotube either directly or through water mediation, where it is damped by the holders (it is also partly absorbed by the reservoir in the Langevin dynamics). In Chart. 1 (bottom), we schematically show the mechanisms of the momentum passage between the ion, water, and nanotube.

In a steady state, the average momentum of each water, p, can be approximately described by the Boltzmann equation

$$\dot{p}_{drag} = \dot{p}_{damp} \propto \frac{p}{\tau_p} \tag{2}$$

where $\dot{p}_{drag}$ and $\dot{p}_{damp}$ are its driving and damping rates, respectively, and τ_p its momentum relaxation time[60,61] (τ_2 in Chart 1). We can assume that $\tau_p^{-1} \approx \tau_{sys}^{-1} + \tau_{Lang}^{-1}$, where the τ_{sys} and τ_{Lang} components are due to (direct and indirect) scattering of water molecules with the nanotube walls and the applied Langevin damping, respectively; we can approximately assume that mutual scattering of molecules flowing in the nanotube does not change their momentum on average.[62] We found that for $\gamma_{Lang} = 0.01$ and 0.02 ps^{-1}, the water dragging velocities, v_w, are very similar, which indicates that $\tau_p \approx \tau_{sys}$ (at this γ_{Lang}). The relaxation time, τ_{sys}, depends on the roughness of the CNT/BNT surfaces, determined by the effective corrugation, C, of the van der Waals (vdW) potential and the nanotube polarity. For simplicity, we can assume that $\tau_{sys} \propto 1/C$.

In a steady state, each water molecule is dragged on average by a force of $F_{drag} = \dot{p}_{drag} \approx q\mathcal{E}/N_w$, where N_w is the number of water molecules in the system. Because $p = m_w v_w = \text{const}$, where m_w is the mass of a single water molecule, we obtain from eq 2 the average velocity of water molecules as

$$v_w \propto \frac{q\mathcal{E}}{N_w m_w C} \tag{3}$$

According to eq 3, v_w is larger in (12,12) CNTs than in (16,16) CNTs by a factor of $v_{w,12}/v_{w,16} \approx N_{w,16}/N_{w,12} = 2$, in rough agreement with our simulation results (Table 1). In BNTs, the corrugation is caused by charged B and N atoms (rather than neutral C atoms); therefore, it is felt deeper, and the difference between the tubes is less significant ($v_{w,12}/v_{w,16} \approx 1.5$). Larger interactions (corrugation) of water molecules with polar BNT walls, $C_{BNT} > C_{CNT}$, should also lead to smaller velocities of water in BNTs, which agrees with the simulations, where $v_{CNT} \approx 4v_{BNT}$.

The above model of the water drag velocities does not capture any differences between the used ions. In order to explain why different ions driven by the same forces drag water differently, we can assume that their momenta are partially relaxed to the nanotube walls in a direct manner without free water playing the intermediate role. Chart 1 shows the mechanisms of ion momentum relaxation in the studied systems. We assume that the hydrated ion is a complex that carries the initial momentum. It can transfer the momentum to free water with a relaxation time τ_1, which passes the momentum further to the nanotube with a relaxation time τ_2. Alternatively, the hydrated ion passes the momentum directly to the nanotube by the relaxation time τ_3. Once the momentum is passed in either way to the nanotube, it can propagate through it in the form of vibrations (phonons), which relax their momenta (directions) at the tube holders (rigid end atoms). In the direct passage of hydrated ion momenta to the nanotubes, we can assume that smaller ions (Na^+) with more rigid hydration shells have a larger direct relaxation to the nanotube walls (small τ_3), while larger ions with "softer" shells relax their momenta more through the free water (small τ_1).

Water Residence Times. We evaluate the residence time of water in the first hydration shell of Na^+ and Cl^-, using the correlation function[63]

$$R(r, t) = \frac{1}{N_r} \sum_{i=1}^{N_r} [\theta(r, 0)\theta(r, t)] \tag{4}$$

where N_r is the average number of water molecules within the first hydration shell of Na^+, Cl^-, and K^+, having radii of $r = 3.2$, 3.8, and 3.7 Å, respectively. Here, $\theta(r, t) = 1$ when the water molecule is in the region of radii $(0, r)$ and is 0 elsewhere, N_r is the number of oxygen atoms in the region $(0, r)$. In Figure 2,

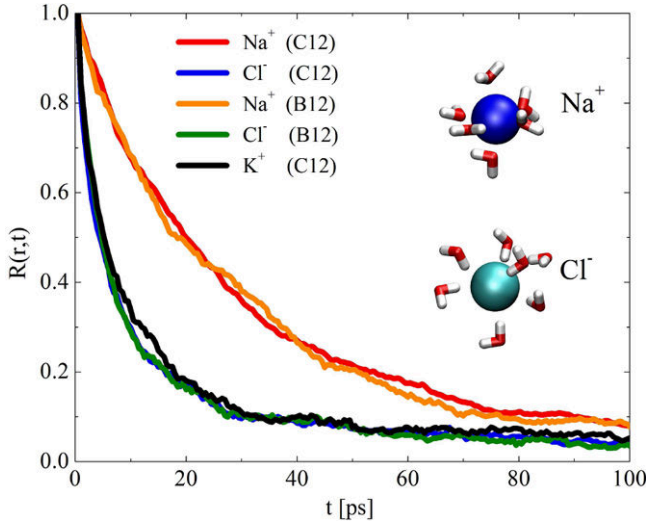


Figure 2. Residence time correlation function, $R(t)$, for water molecules in the first hydration shells of Na^+, Cl^-, and K^+ ions. The plot is shown for the systems containing single ions, passing through the (12,12) CNTs and BNTs, driven as in Chart 1. For K^+, $R(t)$ is not shown for (12,12) BNT for clarity because it is very similar to $R(t)$ in (12,12) CNT. (inset) Snapshots of hydrated Na^+ and Cl^- ions.

we plot $R(r, t)$ for water molecules in the first hydration shells of the Na^+ and Cl^- ions in (12,12) CNT and BNT and of the K^+ ion in (12,12) CNT. The characteristic decay times, τ_i, obtained by fitting $R(r, t)$ to the exponential release rate e^{-t/τ_i}, are $\tau_{Na^+} \approx 30$ ps and $\tau_{Cl^-} \approx 6$ ps in both tubes, which shows that Na^+ binds water molecules more strongly (exchanges them more slowly) than Cl^-.[63] The K^+ ion has $\tau_{K^+} \approx 6$ ps, similar to the Cl^- ion. These decay times correlate well with the fact that Cl^- and K^+ ions are moving faster than Na^+ with respect to water (Δv_i in Table 1). Even though (larger) Cl^- and K^+ ions should move more slowly than Na^+ (Stokes law), their water residence times are shorter; therefore, they can move more

dx.doi.org/10.1021/jz500761s | J. Phys. Chem. Lett. 2014, 5, 2131−2137

easily through water than Na^+ that carries its hydration shell for a longer time.

Distributions of Ion and Water Positions. We can try to estimate how different ions interact with the used nanotubes (directly dissipate momenta) by finding their average distances from the nanotube walls. In Figure 3, we show the normalized

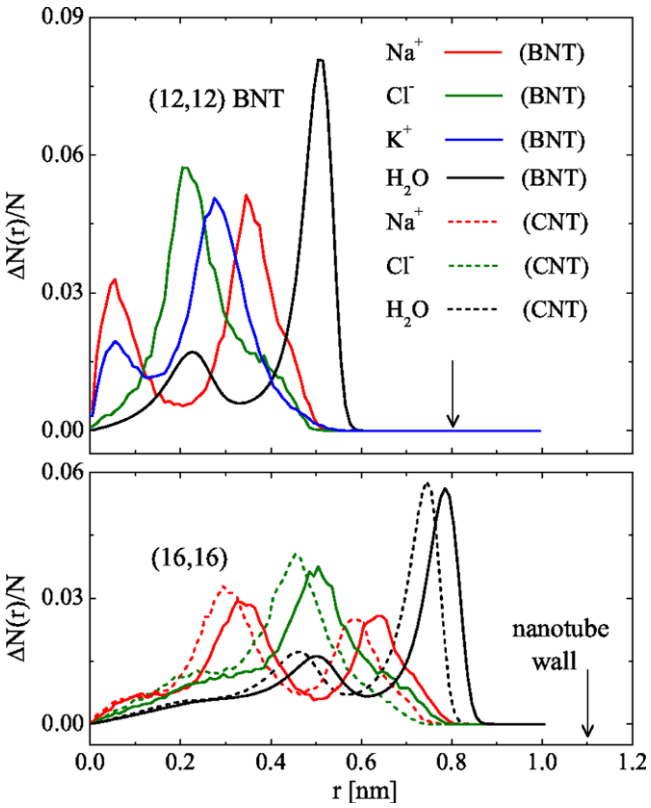


Figure 3. Normalized particle distribution profiles, $\Delta N(r)/N$, of ions and oxygen atoms of water molecules in systems with single Na^+, K^+, and Cl^- ions in the (12,12) BNTs (top) and the (16,16) CNTs and BNTs (bottom). The profiles are obtained by averaging over the whole simulation trajectories.

radial distributions of ions and water oxygens in the systems with single Na^+, K^+, and Cl^- ions solvated in the (12,12) BNTs and (16,16) CNTs and BNTs in the electric field of $\mathcal{E}$ = 0.11 V/nm. The distributions of ions and water molecules, $\Delta N_{i/w}(r)/N_{i/w}$, where r is the distance from the nanotube axis, are obtained by averaging over the whole simulation trajectories.

Notice that in BNTs, all of the distributions are shifted by ~0.05 nm toward the polar walls (shown for (16,16) CNTs and BNTs; a similar shift is observed for (12,12) CNTs and BNTs). Due to water layering,[46] the water (oxygen) distribution has one large peak at 0.3 (0.25) nm from the CNT (BNT) walls and another one shifted by ~0.3 nm and smoothly spreading toward the center of both (12,12) and (16,16) nanotubes. In all of the nanotubes, the Na^+ distribution has two maxima, one between the two water peaks and another one shifted by ~0.3 nm toward the center.[45−47,64] On the other hand, the Cl^- distribution has a single maximum roughly at the position of the second water peak,[37,65] while the K^+ distribution in (12,12) BNTs has a dominant maximum ~0.5 nm from the wall and a small peak toward the nanotube center. In the absence of electric fields, the distributions practically do not change from those shown in Figure 3.

Figure 3 can be simply understood from the fact that Na^+ tends to stay between the oxygen layers, while Cl^- is surrounded by the positive hydrogen atoms. However, K^+ is larger than Na^+, which means that it is more free to move away from the interoxygen region between the two water layers. Using ab initio calculations,[66,67] one can show that the small Na^+ ion can get closer to the CNT or graphene, where a part of its hydration shell is replaced by polarization charges. The electronic response (polarization) of the nanotube is likely to lead to greater damping of the ion and water molecules. In semiconducting CNTs, the polarization would occur mostly along the bonds between nanotube atoms. If so, the CNTs would be more similar to our model of polar BNTs.

Figure 3 can potentially explain the different drag velocities shown in Figure 1 (Table 1). The relaxation time τ_3 associated with a direct transfer of the momentum from the hydrated ion to the nanotube should be shorter when the ion is closer to the nanotube walls (direct friction). The different distances of ions to the tube walls ($r_{Na^+} < r_{K^+} < r_{Cl^-}$) could explain why the v_w water velocities increase in an order of $Na^+ < K^+ < Cl^-$.

Electroosmotic Drag Coefficients. It is of interest to find nanotube electroosmotic drag coefficients, K_{ion}, characterized by the number of water molecules dragged by each ion. The coefficient can be evaluated from $K_{ion} = J_w/J_{ion}$, where $J_w = (N_w/V)\, v_w$ and $J_{ion} = (N_{ion}/V)\, v_i$ are the average water and ion flows, respectively, and N_w (N_{ion}) is the number of water molecules (ions) in the volume V.[68] In bulk solutions, the K_{ion} coefficients roughly correspond to the number of water molecules in the first hydration shells of the involved ions.[68,69] In the nanotube segments with single ions, the number of dragged water molecules is almost 2 orders of magnitude larger than that in bulk ionic solutions[69] (in Table 1, K_{ion} = 260−650). This is due to the inability of water to escape the moving hydrated ion and large slipping of water on the nanotube walls. Therefore, K_{ion} is also by 25−40% larger in CNTs than that in polar BNTs. We observe that K_{Na^+} is by 5−15% larger than K_{Cl^-} and K_{K^+} because the Na^+ complex is more compact (blocking water from escaping). K_{ion} is expected to decrease for larger or longer nanotube segments once the flow is no longer in the regime with the plug-like velocity profile.

Flow in Systems with Neutral Ionic Solutions. Finally, we briefly study the above phenomena in neutral ionic solutions formed by single hydrated ion pairs present in the nanotube segments. In Figure 4, we plot the time dependence for the number of water molecules passing through different nanotubes. We observe a significant electroosmotic flow in (12,12) BNTs for systems containing single (K^+, Cl^-) and (Na^+, Cl^-) pairs and in (16,16) BNTs containing a single (Na^+, Cl^-) pair. In (12,12) BNT containing a (K^+, Cl^-) pair, the Cl^- dominates, but in other cases, the water flow goes in the direction of cations. However, only large flow fluctuations are observed in (16,16) CNTs, which form due to a very small friction between water and CNT walls. While the velocity of water inside of the (16,16) CNT is similar in magnitude to the water velocity inside of the (12,12) and (16,16) BNTs, the flow direction in (16,16) CNT is more random, as seen in Figure 4. In Table 2, we summarize the results for the average ion velocities, v_i, and water velocities, v_w, in the studied systems.

In electric fields, the two ions in these (neutral) systems move in opposite directions; therefore, they meet once during each passage of the nanotube segment. Their average velocities

dx.doi.org/10.1021/jz500761s | J. Phys. Chem. Lett. 2014, 5, 2131−2137

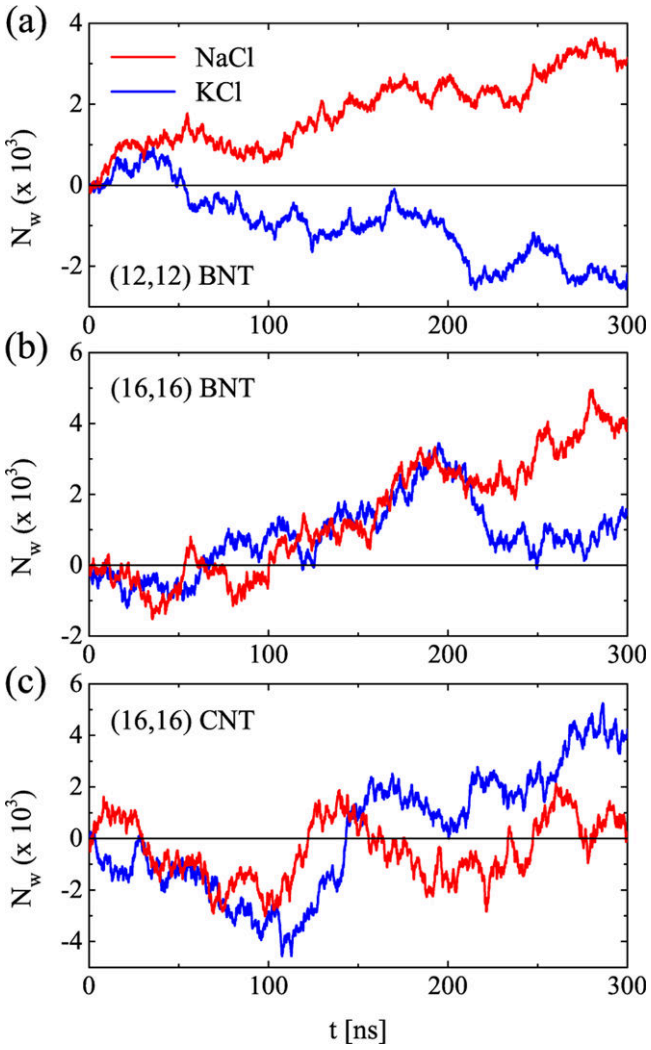


Figure 4. Time dependence of the number of water molecules (N_w) passed through the (12,12) BNTs (top) and (16,16) BNTs (middle) and CNTs (bottom). Systems contain single ion pairs, Na^+ or K^+ cations paired with Cl^- anions, solvated in $N_w \approx 400$ or 800 water molecules that are driven by the electric field of $\mathcal{E} = 0.11$ V/nm. Flow of neutral solutions in (12,12) CNTs was not examined because no differences in water flow were observed for solutions with single ions in (12,12) CNTs (inset of Figure 1).

Table 2. Average Velocities of Cations, Anions (v_i), and Water Molecules (v_w) Obtained in 300 ns Long Simulations of Neutral Solutions in CNTs and BNTs

system, v [nm/ns]	v_i^+	v_i^-	v_w
Na^+Cl^-, B12	5.6	−7.9	**0.24**[a]
C16	8.7	−13.2	0.01
B16	9.6	−13.3	**0.16**
K^+Cl^-, B12	8.4	−8.8	**−0.17**
C16	13.0	−12.8	0.17
B16	13.3	−13.4	0.06

[a]The results highlighted in bold indicate consistent net water flow.

are rather small, and the water drag velocity is nearly zero. Therefore, we cannot expect that the momentum relaxation operates here in the same way as that in the single-ion cases with large velocities of ions and water. Consequently, we cannot assume that a simple superposition of water drag rates from the single-ion cases determines the water drag in the neutral systems. In neutral solutions, other principles can operate. For example, in solution with the Na^+ and Cl^- pair, water driven by the larger Cl^- ion has a larger barrier to pass through the hydrated Na^+ (large rigid shell), while water driven by Na^+ can more easily pass around the soft shell of the hydrated Cl^- ion. Therefore, water is dragged in the direction of Na^+ (Figure 2) rather than in the direction of Cl^-, contrary to our intuition gained from the observation that water moves faster in the single Cl^- case (Figure 1). In solution with K^+ and Cl^- ions, both ions have soft shells; however, Cl^- drags water more (passes more momentum to it); therefore, water goes in its direction.

In previous studies of neutral nanochannels filled with electric-field-driven neutral ionic solutions,[45−47] it was suggested that the observed electroosmotic flows are caused by the existence of a charge double layer at the water−wall interfaces. In the presence of Poiseuille-like velocity profiles of the solution, different ions have different velocities according to their positions in the profile; therefore, they drag water differently. In the presently studied thin nanotubes filled with neutral solutions (Table 2), the ion radial distributions are very similar to those in the single-ion cases, giving charge double layers.[45−47] However, the water velocity profiles inside of thin CNTs and BNTs have plug-like forms,[48] preventing us from using the above explanation of the water drag. We can explain the observed water drag in ultrathin nanochannels filled with neutral ionic solutions by considering a different momentum relaxation between different hydrated ions and nanotubes.

In summary, our MD simulations have revealed that hydrated monovalent ions of different types can drag water at different speeds in thin CNTs and BNTs in the presence of electric fields. When the nanotubes were filled with neutral ionic solutions, we observed electroosmotic flows despite the fact that the nanotubes provide plug-like velocity profiles of the flowing solutions. The efficiency of dragging water was correlated to the momentum relaxation of hydrated ions, depending on their hydration shells and radial distributions in the nanotubes. The described electrokinetic phenomena can have a broad range of applications in molecular separation, desalination, and nanofluidics.

AUTHOR INFORMATION

Corresponding Author

*E-mail: pkral@uic.edu.

Notes

The authors declare no competing financial interest.

ACKNOWLEDGMENTS

This work was supported by a grant from the NSF (CBET-0932812). E.V. acknowledges the generous support from the Herbert E. Paaren Summer Research Fellowship and Academic Year Research Award, and L.V. acknowledges the support through the UIC Dean Scholar Award. We acknowledge the computer time provided by the NERSC (award M1201), XSEDE (award CHE060021N), and CNM supercomputing centers.

REFERENCES

(1) Storm, A. J.; Chen, J. H.; Ling, X. S.; Zandbergen, H. W.; Dekker, C. Fabrication of Solid-State Nanopores with Single-Nanometre Precision. *Nat. Mater.* **2003**, *2*, 537−540.

(2) Jágerszki, G.; Gyurcsányi, R. E.; Höfler, L.; Pretsch, E. Hybridization-Modulated Ion Fluxes through Peptide-Nucleic-Acid-Functionalized Gold Nanotubes. A New Approach to Quantitative Label-Free DNA Analysis. *Nano Lett.* **2007**, *7*, 1609−1612.
(3) King, T. L.; Gatimu, E. N.; Bohn, P. W. Single Nanopore Transport of Synthetic and Biological Polyelectrolytes in Three-Dimensional Hybrid Microfluidic/Nanofluidic Devices. *Biomicrofluidics* **2009**, *3*, 012004.
(4) Das, G.; Talukdar, P.; Matile, S. Fluorometric Detection of Enzyme Activity with Synthetic Supramolecular Pores. *Science* **2002**, *298*, 1600−1602.
(5) Titov, A. V.; Wang, B.; Sint, K.; Král, P. Controllable Synthetic Molecular Channels: Biomimetic Ammonia Switch. *J. Phys. Chem. B* **2009**, *114*, 1174−1179.
(6) Král, P.; Shapiro, M. Nanotube Electron Drag in Flowing Liquids. *Phys. Rev. Lett.* **2001**, *86*, 131−134.
(7) Ghosh, S.; Sood, A. K.; Kumar, N. Carbon Nanotube Flow Sensors. *Science* **2003**, *299*, 1042−1044.
(8) Wang, B.; Král, P. Coulombic Dragging of Molecules on Surfaces Induced by Separately Flowing Liquids. *J. Am. Chem. Soc.* **2006**, *128*, 15984−15985.
(9) Wang, B.; Král, P. Dragging of Polarizable Nanodroplets by Distantly Solvated Ions. *Phys. Rev. Lett.* **2008**, *101*, 046103.
(10) Hummer, G.; Rasaiah, J. C.; Noworyta, J. P. Water Conduction through the Hydrophobic Channel of a Carbon Nanotube. *Nature* **2001**, *414*, 188−190.
(11) Majumder, M.; Chopra, N.; Andrews, R.; Hinds, B. J. Nanoscale Hydrodynamics: Enhanced Flow in Carbon Nanotubes. *Nature* **2005**, *438*, 44.
(12) Whitby, M.; Quirke, N. Fluid Flow in Carbon Nanotubes and Nanopipes. *Nat. Nanotechnol.* **2007**, *2*, 87−94.
(13) Wu, J.; Zhan, X.; Hinds, B. J. Ionic Rectification by Electrostatically Actuated Tethers on Single Walled Carbon Nanotube Membranes. *Chem. Commun.* **2012**, *48*, 7979−7981.
(14) Král, P.; Wang, B. Material Drag Phenomena in Nanotubes. *Chem. Rev.* **2013**, *113*, 3372−3390.
(15) Won, C. Y.; Aluru, N. R. Water Permeation through a Subnanometer Boron Nitride Nanotube. *J. Am. Chem. Soc.* **2007**, *129*, 2748−2749.
(16) Sint, K.; Wang, B.; Král, P. Selective Ion Passage through Functionalized Graphene Nanopores. *J. Am. Chem. Soc.* **2008**, *130*, 16448−16449.
(17) Garaj, S.; Hubbard, W.; Reina, A.; Kong, J.; Branton, D.; Golovchenko, J. A. Graphene as a Subnanometre Trans-Electrode Membrane. *Nature* **2010**, *467*, 190−193.
(18) Yzeiri, I.; Patra, N.; Král, P. Porous Carbon Nanotubes: Molecular Absorption, Transport, and Separation. *J. Chem. Phys.* **2014**, *140*, 104704−1−5.
(19) Lee, C. Y.; Choi, W.; Han, J.-H.; Strano, M. S. Coherence Resonance in a Single-Walled Carbon Nanotube Ion Channel. *Science* **2010**, *329*, 1320−1324.
(20) van der Heyden, F. H. J; Bonthuis, D. J.; Stein, D.; Meyer, C.; Dekker, C. Power Generation by Pressure-Driven Transport of Ions in Nanofluidic Channels. *Nano Lett.* **2007**, *7*, 1022−1025.
(21) Siria, A.; Poncharal, P.; Biance, A.-L.; Fulcrand, R.; Blase, X.; Purcell, S. T.; Bocquet, L. Giant Osmotic Energy Conversion Measured in a Single Transmembrane Boron Nitride Nanotube. *Nature* **2013**, *494*, 455−458.
(22) Cheng, L.-J.; Guo, L. J. Rectified Ion Transport through Concentration Gradient in Homogeneous Silica Nanochannels. *Nano Lett.* **2007**, *7*, 3165−3171.
(23) Kuo, T.-C.; Sloan, L. A.; Sweedler, J. V.; Bohn, P. W. Manipulating Molecular Transport through Nanoporous Membranes by Control of Electrokinetic Flow: Effect of Surface Charge Density and Debye Length. *Langmuir* **2001**, *17*, 6298−6303.
(24) Harrell, C. C.; Kohli, P.; Siwy, Z.; Martin, C. R. DNA−Nanotube Artificial Ion Channels. *J. Am. Chem. Soc.* **2004**, *126*, 15646−15647.
(25) Li, N.; Yu, S.; Harrell, C. C.; Martin, C. R. Conical Nanopore Membranes. Preparation and Transport Properties. *Anal. Chem.* **2004**, *76*, 2025−2030.
(26) Ramirez, P.; Gomez, V.; Cervera, J.; Schiedt, B.; Mafe, S. Ion Transport and Selectivity in Nanopores with Spatially Inhomogeneous Fixed Charge Distributions. *J. Chem. Phys.* **2007**, *126*, 194703.
(27) Li, Y.; Maire, H. C.; Ito, T. Electrochemical Characterization of Nanoporous Films Fabricated from a Polystyrene−Poly(methylmethacrylate) Diblock Copolymer: Monitoring the Removal of the PMMA Domains and Exploring the Functional Groups on the Nanopore Surface. *Langmuir* **2007**, *23*, 12771−12776.
(28) Baldessari, F.; Santiago, J. G. Electrophoresis in Nanochannels: Brief Review and Speculation. *J. Nanobiotechnol.* **2006**, *4*, 12.
(29) Daiguji, H. Ion Transport in Nanofluidic Channels. *Chem. Soc. Rev.* **2010**, *39*, 901−911.
(30) Dukhin, S. S.; Derjaguin, B. V. *Electrokinetic Phenomena*; John Wiley and Sons: New York, 1974.
(31) Kim, Y. W.; Netz, R. R. Electro-osmosis at Inhomogeneous Charged Surfaces: Hydrodynamic versus Electric Friction. *J. Chem. Phys.* **2006**, *124*, 114709/1−114709/21.
(32) Kirby, B. J. *Micro- and Nanoscale Fluid Mechanics: Transport in Microfluidic Devices*; Cambridge University Press: Cambridge, U.K., 2010.
(33) Harrison, D. J.; Fluri, K.; Seiler, K.; Fan, Z.; Effenhauser, C. S.; Manz, A. Micromachining a Miniaturized Capillary Electrophoresis-Based Chemical Analysis System on a Chip. *Science* **1993**, *261*, 895−897.
(34) Patankar, N. A.; Hu, H. H. Numerical Simulation of Electroosmotic Flow. *Anal. Chem.* **1998**, *70*, 1870−1881.
(35) Herr, A. E.; Molho, J. I.; Santiago, J. G.; Mungal, M. G.; Kenny, T. W.; Garguilo, M. G. Electroosmotic Capillary Flow with Nonuniform Zeta Potential. *Anal. Chem.* **2000**, *72*, 1053−1057.
(36) Liu, H.; He, J.; Tang, J.; Liu, H.; Pang, P.; Cao, D.; Krstic, P.; Joseph, S.; Lindsay, S.; Nuckolls, C. Translocation of Single-Stranded DNA through Single-Walled Carbon Nanotubes. *Science* **2010**, *327*, 64−67.
(37) Kim, D.; Darve, E. Molecular Dynamics Simulation of Electro-osmotic Flows in Rough Wall Nanochannels. *Phys. Rev. E* **2006**, *73*, 051203.
(38) Suk, M. E.; Raghunathan, A. V.; Aluru, N. R. Fast Reverse Osmosis Using Boron Nitride and Carbon Nanotubes. *Appl. Phys. Lett.* **2008**, *92*, 133120.
(39) Noy, A.; Park, H. G.; Fornasiero, F.; Holt, J. K.; Grigoropoulos, C. P.; Bakajin, O. Nanofluidics in Carbon Nanotubes. *Nano Today* **2007**, *2*, 22−29.
(40) Li, J.; Gong, X.; Lu, H.; Li, D.; Fang, H.; Zhou, R. Electrostatic Gating of a Nanometer Water Channel. *Proc. Natl. Acad. Sci. U.S.A.* **2007**, *104*, 3687−3692.
(41) Karnik, R.; Fan, R.; Yue, M.; Li, D.; Yang, P.; Majumdar, A. Electrostatic Control of Ions and Molecules in Nanofluidic Transistors. *Nano Lett.* **2005**, *5*, 943−948.
(42) Qiao, R.; Aluru, N. R. Atypical Dependence of Electroosmotic Transport on Surface Charge in a Single-Wall Carbon Nanotube. *Nano Lett.* **2003**, *3*, 1013−1017.
(43) Qiao, R.; Aluru, N. R. Charge Inversion and Flow Reversal in a Nanochannel Electro-osmotic Flow. *Phys. Rev. Lett.* **2004**, *92*, 198301.
(44) Pang, P.; He, J.; Park, J. H.; Krstić, P. S.; Lindsay, S. Origin of Giant Ionic Currents in Carbon Nanotube Channels. *ACS Nano* **2011**, *5*, 7277−7283.
(45) Dukhin, A.; Dukhin, S.; Goetz, P. Electrokinetics at High Ionic Strength and Hypothesis of the Double Layer with Zero Surface Charge. *Langmuir* **2005**, *21*, 9990−9997.
(46) Joseph, S.; Aluru, N. R. Hierarchical Multiscale Simulation of Electrokinetic Transport in Silica Nanochannels at the Point of Zero Charge. *Langmuir* **2006**, *22*, 9041−9051.
(47) Kim, D.; Darve, E. High-Ionic-Strength Electroosmotic Flows in Uncharged Hydrophobic Nanochannels. *J. Colloid Interface Sci.* **2009**, *330*, 194−200.

(48) Joseph, S.; Aluru, N. R. Why Are Carbon Nanotubes Fast Transporters of Water? *Nano Lett.* **2008**, *8*, 452−458.
(49) Joseph, S.; Mashl, R. J.; Jakobsson, E.; Aluru, N. R. Electrolytic Transport in Modified Carbon Nanotubes. *Nano Lett.* **2003**, *3*, 1399−1403.
(50) Liu, H.; Murad, S.; Jameson, C. J. Ion Permeation Dynamics in Carbon Nanotubes. *J. Chem. Phys.* **2006**, *125*, 084713.
(51) Hilder, T. A.; Gordon, D.; Chung, S.-H. Boron Nitride Nanotubes Selectively Permeable to Cations or Anions. *Small* **2009**, *5*, 2870−2875.
(52) Hilder, T. A.; Gordon, D.; Chung, S.-H. Salt Rejection and Water Transport through Boron Nitride Nanotubes. *Small* **2009**, *5*, 2183−2190.
(53) Fornasiero, F.; Park, H. G.; Holt, J. K.; Stadermann, M.; Grigoropoulos, C. P.; Noy, A.; Bakajin, O. Ion Exclusion by Sub-2-nm Carbon Nanotube Pores. *Proc. Natl. Acad. Sci. U.S.A.* **2008**, *105*, 17250−17255.
(54) Corry, B. Designing Carbon Nanotube Membranes for Efficient Water Desalination. *J. Phys. Chem. B* **2007**, *112*, 1427−1434.
(55) Phillips, J. C.; Braun, R.; Wang, W.; Gumbart, J.; Tajkhorshid, E.; Villa, E.; Chipot, C.; Skeel, R. D.; Kale, L.; Schulten, K. Scalable Molecular Dynamics with NAMD. *J. Comput. Chem.* **2005**, *26*, 1781−1802.
(56) Humphrey, W.; Dalke, A.; Schulten, K. VMD: Visual Molecular Dynamics. *J. Mol. Graph.* **1996**, *14*, 33−38.
(57) MacKerell, A. D.; Bashford, D.; Bellott; Dunbrack, R. L.; Evanseck, J. D.; Field, M. J.; Fischer, S.; Gao, J.; Guo, H.; Ha, S.; Joseph-McCarthy, D.; et al. All-Atom Empirical Potential for Molecular Modeling and Dynamics Studies of Proteins. *J. Phys. Chem. B* **1998**, *102*, 3586−3616.
(58) Won, C. Y.; Aluru, N. R. Structure and Dynamics of Water Confined in a Boron Nitride Nanotube. *J. Phys. Chem. C* **2008**, *112*, 1812−1818.
(59) Darden, T.; York, D.; Pedersen, L. Particle mesh Ewald: An N·log(N) Method for Ewald Sums in Large Systems. *J. Chem. Phys.* **1993**, *98*, 10089−10092.
(60) Bhatnagar, P. L.; Gross, E. P.; Krook, M. A Model for Collision Processes in Gases. I. Small Amplitude Processes in Charged and Neutral One-Component Systems. *Phys. Rev.* **1954**, *94*, 511−525.
(61) Vuković, L.; Král, P. Coulombically Driven Rolling of Nanorods on Water. *Phys. Rev. Lett.* **2009**, *103*, 246103.
(62) Král, P. Linearized Quantum Transport Equations: ac Conductance of a Quantum Wire with an Electron−Phonon Interaction. *Phys. Rev. B* **1996**, *53*, 11034−11050.
(63) Lee, S. H.; Rasaiah, J. C. Molecular Dynamics Simulation of Ion Mobility. 2. Alkali Metal and Halide Ions Using the SPC/E Model for Water at 25°. *J. Phys. Chem.* **1996**, *100*, 1420−1425.
(64) Mucha, M.; Frigato, T.; Levering, L. M.; Allen, H. C.; Tobias, D. J.; Dang, L. X.; Jungwirth, P. Unified Molecular Picture of the Surfaces of Aqueous Acid, Base, and Salt Solutions. *J. Phys. Chem. B* **2005**, *109*, 7617−7623.
(65) Qiao, R.; Aluru, N. R. Ion Concentrations and Velocity Profiles in Nanochannel Electroosmotic Flows. *J. Chem. Phys.* **2003**, *118*, 4692−4701.
(66) Leung, K.; Marsman, M. Energies of Ions in Water and Nanopores within Density Functional Theory. *J. Chem. Phys.* **2007**, *127*, 154722.
(67) Patra, N.; Esan, D. A.; Král, P. Dynamics of Ion Binding to Graphene Nanostructures. *J. Phys. Chem. C* **2013**, *117*, 10750−10754.
(68) Yan, L.; Shao, C.; Ji, X. Evaluation of Electroosmotic Drag Coefficient of Water in Hydrated Sodium Perfluorosulfonate Electrolyte Polymer. *J. Comput. Chem.* **2009**, *30*, 1361−1370.
(69) Yan, L.; Ji, X.; Lu, W. Molecular Dynamics Simulations of Electroosmosis in Perfluorosulfonic Acid Polymer. *J. Phys. Chem. B* **2008**, *112*, 5602−5610.